Assessment of rheological and sedimentation characteristics of fresh cemented tailings backfill slurry

Shuai Cao[1, 2, 3], Gaili Xue[1, 2], Erol Yilmaz[4, *], Zhenyu Yin[3]

1. State Key Laboratory of High-Efficient Mining and Safety of Metal Mines of Ministry of Education, University of Science and Technology Beijing, Beijing 100083, China

2. School of Civil and Resource Engineering, University of Science and Technology Beijing, Beijing 100083, China

3. Department of Civil and Environmental Engineering, The Hong Kong Polytechnic University, Hung Hom, Kowloon, Hong Kong, China

4. Department of Civil Engineering, Geotechnical Division, Recep Tayyip Erdogan University, Fener, Rize TR53100, Turkey

**Corresponding author:* erol.yilmaz@erdogan.edu.tr (E. Yilmaz)

E-mail addresses: sandy_cao@ustb.edu.cn (S. Cao); hnpyxgl@126.com (GL. Xue); zhenyu.yin@polyu.edu.hk (ZY. Yin)

Abstract: The rheological characteristics of cemented tailings backfill (CTB) are crucial for pipeline transportation since large quantities of backfilling can be fast delivered over long distances at relatively low costs, thereby resulting high backfilling rate and high mining circle. Unreasonable choice of solid content (SC) and cement-to-tailings ratio (c/t), including pipeline networking system, will lead to some pipeline problems, such as blockage, wear, and rupture. Hence, this study deals with the rheological behavior and sedimentation characteristics of fresh CTB slurry. Samples having a SC value of 65, 67 and 69wt.%, as well as a c/t ratio of 1:2, 1:1 and 1:4, were prepared and exposed to their rheological tests. Likewise, the sedimentation properties of CTB slurry was studied by picking polyacrylamide (PAM) as flocculant. Results showed that: (1) CTB's slump reduced with growing SC and c/t values when SC was kept constant. (2) The viscosity and shear stress increased with increasing SC values, signifying a linear link between shear stress and stress rate. (3) There was also an exponential link between sedimentation rate and PAM flocculant content in CTB material. The sedimentation rate with a high PAM content was hugely faster than other groups at the initial stage of the sedimentation of tailings slurry. When PAM value increased from 75 to 80 g/t, a clear difference was observed in the clarification layer height (CLH). Besides, the CLH increments were 7.5 and 7.14% for a ST of 20 and 30 min, respectively. Thus, the outcomes of this work propose a scientific reference to the mining industry in considering the transport aspect of CTB slurry to underground mined-out stopes.

Keywords: Cemented tailings backfill; sedimentation characteristics; rheological behavior; flocculant; slump; viscosity; solid content; cement-to-tailings ratio

1 Introduction

Global demand is growing for mineral resources of metals and industrial minerals which provide a main matrix foundation for human civilization [1]. Mining is one of the commonly used approaches to extract run-of-mine ores safely; but can result in lots of environmental damage, such as land subsidence, underground water pollution [2,3]. Besides, large voluminous solid wastes, also known as tailings, are unavoidably generated after mineral processing [4,5]. At present, the tailings treatment methods principally include tailings dam stacking, backfilling underground mined-out area, preparation of construction materials, and active mining subsidence areas control [6-9]. Moreover, backfill methods can also be used as an efficient waste-disposal system within mined-out rooms [10-14]. Underground mines in deep, high-stress, and soft-rock ground conditions need backfilling of mined-out areas to offer local and regional ground support to the host rock mass [15,16]. Generally, the materials used for backfilling at most underground mines consist typically of processing tailings, alluvial sands, coal gangue-fly ash, crushed waste rocks, and smelter slags from underground or open-pit coal, metal and non-metal mining [17-23]. When compared to other types of filling such as rock backfill, slurry fill, and coal fly ash backfill, cemented paste or tailings backfill (CPB or CTB) is gaining popularity in mines due to its fast backfill rates, no water removal requirement from the stope, and non-segregating and -desliming tailings backfilling [24-26].

CTB is an engineered, non-Newtonian fluid, and pumpable mixture that regularly consists of wet filter tailings, hydraulic cement (rarely mineral/chemical additives), and mixing water for safe transport in the pipeline due to its high percent solids concentration (e.g., 65-85wt% by dry tailings) and fines content (15-75% minus 20 μm) [27-30]. After being stirred at the land backfilling station, the fresh CTB slurry discharges from a plastic pipe at the end of transportation and is poured into a mined-out stope from the top corner while the bottom side of the filled-stope is constructed by a barricade [31,32]. Fig. 1. shows a basic delivery system of CTB, based on its own gravity or pumped. Essentially, the delivery of CTB to underground stopes inevitably results in high pipe wear rates which may increase maintenance costs, cause operational downtimes, and affect the flow profile of the paste material [33-35]. A review of the factors affecting the pipe wears indicates that the velocity or filling rate is considered to be a leading factor, with other important factors involving the material characteristics (e.g., solid content, corrosive minerals, particle shape, and gradation) of the CTB delivered, the pipeline network system, and the flow regime [36-39]. Hence, the transport of CTB with high-density slurries needs to be further understood for better underground mine fill design from the operational and financial points of view.

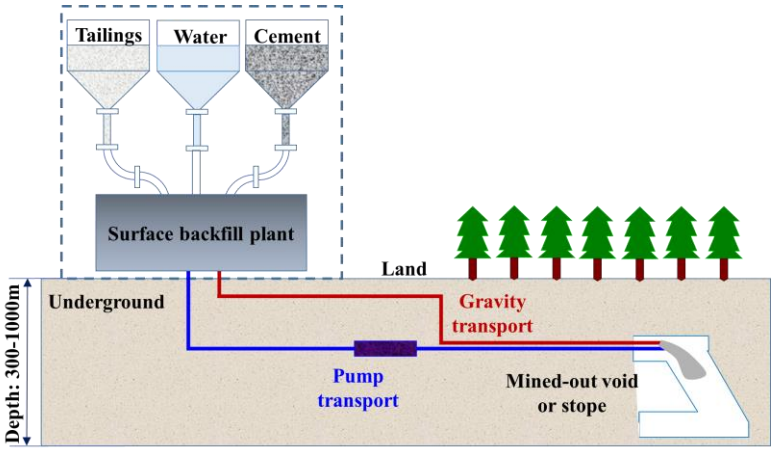

Fig. 1 Backfill slurry transportation into underground mined-out stopes

Until now, numerous researchers have focused on macro-mechanical characteristics of CTB materials as follows: uniaxial and triaxial compression, dynamic characteristics, splitting, and three-point bending [13, 32, 37, 40-43]. To explore the relations between the macro-mechanical behavior of the backfill and the internal porosity, a number of different non-destructive test methods have also been used for CTB investigations, such as ultrasonic velocity, nuclear magnetic resonance, acoustic emission, and industrial computer tomography [37, 39, 41, 44-49]. Xue et al. [32] found that if porosity gets below 0.2%, the strength gain of cemented-tailings matrix composites (CTMC) reinforced with fiber reinforcement is less influenced by the intrinsic structure-property. They have also shown that defining a relationship between strength development and the internal structure of filling through X-ray CT is achievable.

For pipeline design purposes, the rheology (e.g., yield stress and viscosity) of fresh fill slurries is also another important aspect to be considered for underground backfilling and therefore, the influence of some index factors on its rheological behavior was studied earlier by some researchers [30, 33, 50-52]. Bian et al. [53] assessed sulfate effect on yield stress and viscosity of fiber-reinforced fill and showed that viscosity rises while yield stress reduces with increasing sulphate content. They concluded that sulphate ions influence the hydration products and the zeta potential of backfill with fiber reinforcement. Jiang and Fall [54] examined the sodium chloride (NaCl) effect on the yield stress of slag-contained backfill cured at -6 °C and indicated that adding NaCl into backfill improves its flowability and strength development. A surge in the salinity of pore fluid gives rise to a drop in yield stress and strength of backfilling. High salinity content is closely related to additional water within the backfill, causing a reduction in the strength of filling. Jiang and Fall [55] also studied the development of yield stress and mechanical behavior of Portland cement-contained fill with different saline contents. They commented that yield stress reduces with mounting salinity owing to adsorption of chloride ions into cement particle

surface and hydration products (e.g., high zeta potential values). Moreover, Wu et al. [56] investigated changes in rheological characteristics of filling under temperature and hydration effects. They demonstrated that temperature and progress of cement hydration play a key role in rheological behavior and flowability. The yield stress of filling rises with increasing temperature, and curing time rises. The viscosity of filling also rises as the time of hydration or the temperature within the backfill rises, which is really important for the transport of filling into underground mined-out stopes.

In essence, CTB slurry is a solid-liquid-gas three-phase fluid that composes of air, water, tailings, and gel materials. The flow properties of CTB include slump, sedimentation rate, yield stress, viscosity, bleeding rate [30, 34, 57-61]. Besides, several researchers have used additives to alter CTB's rheology, such as high-calcium sepiolite, sulfate, superplasticizers, styrene-butadiene rubber latex [62-70]. Feys et al. [71] found that the structural failure happens principally when shifted from the rest to lower shear rates; nevertheless, several networks are destructed at higher shear rates. Jiao et al. [72] also found that the act of shear mixing decelerated the progress of thixotropy, but the efficacy of drop was steadily restricted. Deng et al. [33, 51] thought that specimens sheared at higher rates show lesser viscosity values compared to ones sheared at lower rates. Jiang et al. [52] analyzed the yield stress of fill being cured under sub-zero temperatures and found that the yield stress of fills exposed to sub-zero temperatures is under the ones cured in chamber temperature. Sedimentation is defined as the affinity for grains in suspension to settle out of the fluid in which they are kept and arise to repose against an obstacle. The sedimentation behavior of cementitious materials, such as CTB and mortar, is greatly affected by some factors: density differences, viscous flow of liquid, dissolution, shrinkage, thixotropic, and admixtures [25, 73-75]. Note that the sedimentation property of coarse sized tailings backfill is relatively high when compared to the CTB matrix with fine grain size [76-79]. However, coarse grain sizes can cause pipe-blockages, damaging the efficiency and operation of CTB [80]. Consequently, the sedimentation characteristics of CTB materials need to be better investigated in every aspect.

The novelty of the present study is the appraisal of solid content (SC) and cement/tailings (c/t) ratio effects on rheological behavior and sedimentation property of CTB. It will mature our considerate of the influence of rheology and sedimentation, which affect both flow and transport properties of filling. This study also presents the findings of the flocculation characteristics in order to demonstrate the flocculation efficiency of polyacrylamide, which is a polymer employed for treating water thanks to its high efficacy and quick dissolution. The flocculation properties were evaluated by using a polymer dosage of 60-95 g/t at room temperature.

2 Materials and Methods

2.1 Materials

2.1.1 Process tailings

Collected for CTB production from an Au mine in the province of Gansu, Northwest China, tailings are categorized as unclassified products. The tailings' grain size distribution (GSD) was determined by employing an SA-CP3 laser grain sizer (which measures grains changing from 0.02 to 2000 μm with a ±1% precision). One can see from the acquired GSD curves, as shown in Fig. 2, that more than 50% of the gold tailings particles are smaller than 38.33μm (d_{50}). Besides, the d_{10}, d_{30} and d_{60} are 2.8μm, 10.76μm and 55.02μm, respectively. GSD results verify that the studied tailings specimen had a quite varied range and a flat continuous distribution. Tailings' chemical composition is chiefly silicon dioxide (SiO_2: 54.2%), aluminum oxide (Al_2O_3: 13%), calcium oxide (CaO: 6.59%) and magnesium oxide (MgO: 1.77%). Alkalinity and activity rate of tailings are also found to be 0.124 and 0.24, respectively.

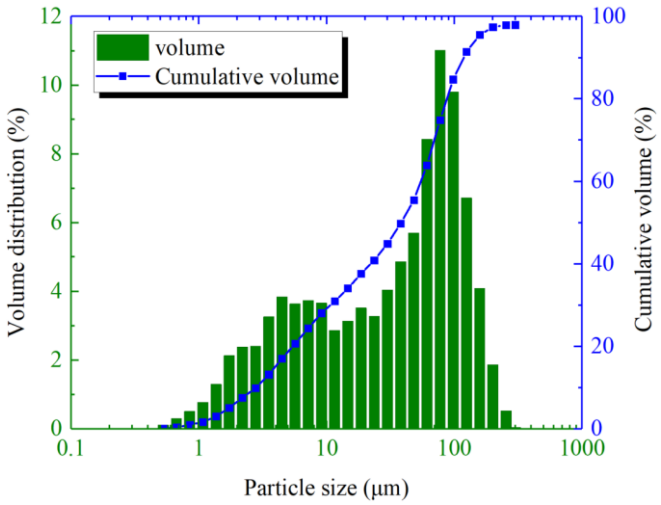

Fig. 2 GSD curves of the tested gold tailings

2.1.2 Cement and mixing water

Ordinary Portland cement (P.O. 42.5R) was utilized as the main binder. Some physical property results indicated that the Blaine fineness of P.O. 42.5R cement is 405 m^2/kg, the specific gravity (SG) is 3.14, and the initial setting time (IST) is 120 min. The chemistry of P.O. 42.5R was presented in Table 1. It was found that CaO and SiO_2 are the main components and their contents are 61.8% and 20.1%, respectively. As for mixing water, municipal water was employed to blend both gold tailings and P.O. 42.5R cement consistently. It should be emphasized that the effect of municipal water on backfill chemistry is not considered in the present study.

Table 1 Oxide analysis of ordinary Portland cement (P.O. 42.5R) employed in the experiments.

Varieties (%)	SiO_2	Fe_2O_3	Al_2O_3	MgO	CaO	SO_3	K_2O
P.O. 42.5R	20.1	2.91	5.11	1.57	61.8	1.98	0.37

2.2 CTB slurry preparation

In this study, three types of c/t ratio values (e.g., 1:4, 1:10 and 1:20) were considered to measure the rheological behavior of fresh CTB slurry. Besides, three kinds of solid content values (e.g., 65, 67, and 69wt.%) were also selected for the preparation of CTB slurry. Fig. 3 demonstrates the preparation of three different CTB slurries. An industry-type mixer was used for the homogenization of the backfill mixtures. Note that all CTB samples were prepared by mixing at least 5 minutes and tested in various situations at room temperature (25±1°C).

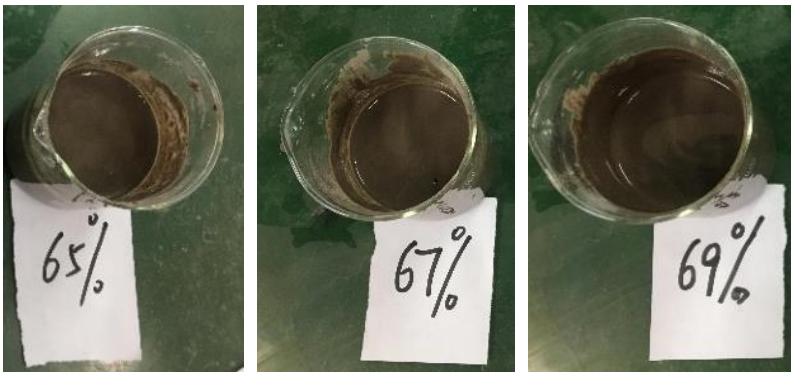

Fig. 3 The slurry preparation of three different density CTB mixtures

2.3 Slump tests

The slump, which is defined as the measure of the drop of fill when it is done by using a standard Abraham cone, is one of the important index tests to judge the flow performance of CTB slurry better. A standard cone of 300 mm was used to investigate the slump values of CTB slurry. This cone has a 100-mm top ring diameter, a 200-mm bottom ring diameter, and a 300-mm height. Firstly, CTB slurries are poured into a cone at 3 layers. Each layer of CTB was tamped 25 times along the spiral from the edge to the center. After inserting and tamping, the excess slurry was scraped off and smoothed to remove the mortar on the sides of the top ring. Second, the slump cone was lifted up vertically and steadily, and the lifting process of the tube should not be interrupted. Note that the time for pulling up the slump cone must be completed in 5-10 seconds. Third, the height between the top ring and the highest point of CTB slurry was measured, and the obtained data were recorded for the evaluation of the slump test results.

2.4 Sedimentation tests

Pumps, which have to aptly operate a 20% flow rate larger than the design flow rate for the solids-water system, are needed for the underground delivery of CTB slurries. The falling in the flow rate to the critical sedimentation value gives rise to a whole pipe filling. The flow of CTB slurries is thoroughly related to the slump and sedimentation of fresh fill material. Polyacrylamide (PAM), a type of chelating polymer, was selected as flocculant. The basic parameters of this test were shown as follows: relative molecular weight, ionicity, bulk density, and viscosity were 10,000,000, anionic, 0.70 gms/cm^3 and 950 mPa·s. In this study, a total of 8 different dosage rates of PAM were used as 60, 65, 70, 75, 80, 85, 90, and 95g/t, respectively.

According to the sedimentation law of the gold tailings samples in the vertical sand silo, through the flocculation sedimentation experiment of each mortar in experiments, it was found that the solid-liquid separation interface was clearly visible when sedimentation was about 1 min. The mortar sedimentation rate was calculated after adding flocculant, as follows:

$$V = \frac{H_0 - H_1}{t}$$

Where, V is the sedimentation rate (cm/min); H_o is the initial height of the sedimentation level; H_1 is the height of the sedimentation level at a sedimentation of 1min; t is sedimentation time.

2.5 Rheological tests

To define the rheological parameters (e.g., yield stress and viscosity) of the backfill featuring c/t and SC, a rheometer (Brookfield R/S+SST) equipped with a V40-20 vane rotor was employed at the laboratory. The experimental data were delivered into PC and computed with code (Fig. 4). It has a clear advantage of eliminating the wall-slip influence with no damage to the flocculent creation of CTB [81]. Note that the 4-paddle rotor was immersed into the CTB matrix, rotating at diverse velocities to produce various shear rates. The backfill mix was put to a beaker, which has a 95 mm diameter and a 115 mm height. The temperature of the water bath is kept constant at 19.2 ℃. Shear rate changes between 0 and 200 s^{-1}. The test time was set to 200 secs, and the measurement step is 1 sec.

CTB's rheology has constitutive relations which are determined by the Herschel-Bulkley flow model [52]. This model mainly deals with relationship between shear stress and shear rate, which entirely covers the shear stresses measured from the commencement of the backfill flow.

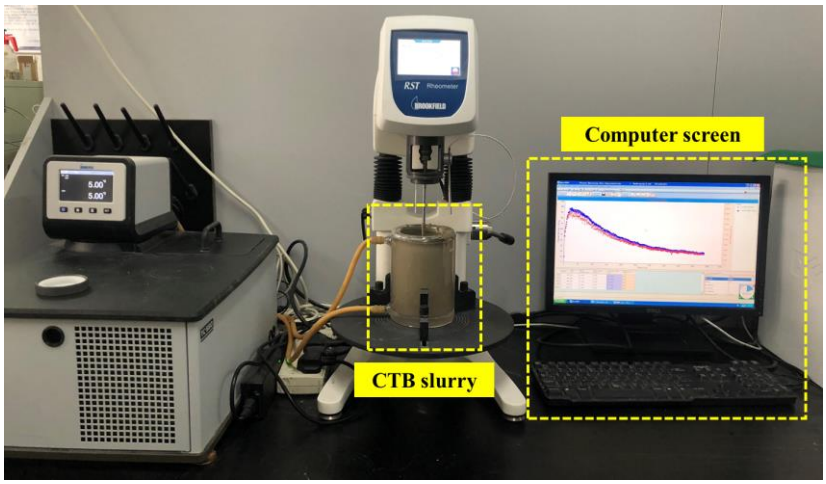

Fig. 4 A photograph of the rheological testing device

3 Results and Discussions

3.1 Slump property of CTB slurry

Fig. 5 indicates the histogram curve between CTB slurry slump and solid content (SC). Overall, the slump values of CTB slurry decrease with increasing SC values chiefly attributable to a weighty drop in the corresponding moisture within the filling. A drop in the workability is principally caused by the water molecules being absorbed by cement-tailings particles. Note that a slump value of not less than 15 cm should be practiced in order to get the backfill pumped to mine voids through pipelines. The high solid content may cause pipe blockages even though it helps to increase the corresponding backfill strength. In-situ fill applications, the solid content of filling is augmented in order to improve its strength gaining. Nevertheless, the process is followed to guarantee the necessity of fill workability.

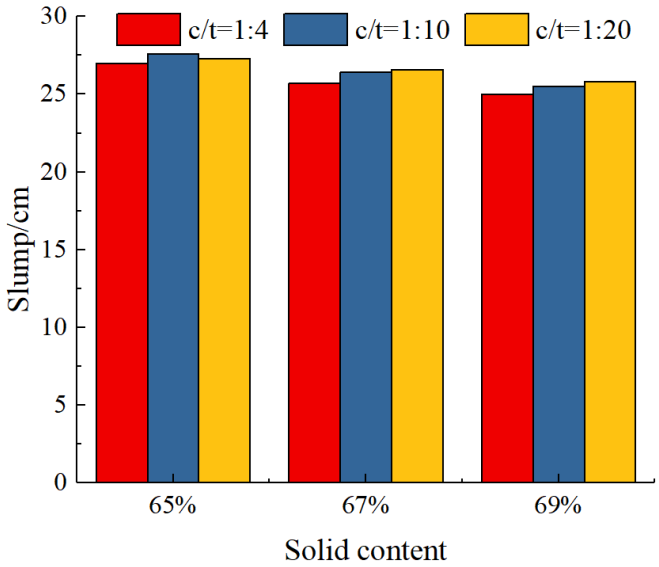

Fig. 5 Change in the backfill slump considering SC and c/t ratio

The slump values also reduce with growing c/t value for a given SC value. For instance, as the solid content rises from 65 to 69 wt.%, the corresponding slump values reduce slowly, exhibiting no sharp change in the slump. This is closely related to the material property of tailings and the used cement fineness. As the particle sizes of gold tailings are very close to that of P.O. 42.5R, the mixing water is equivalently disseminated on the surface of tailings and cement fine particles. There will be no vital variation in the slump rise or drop of CTB slurry when there is no effect of curing conditions, such as high temperatures and stresses.

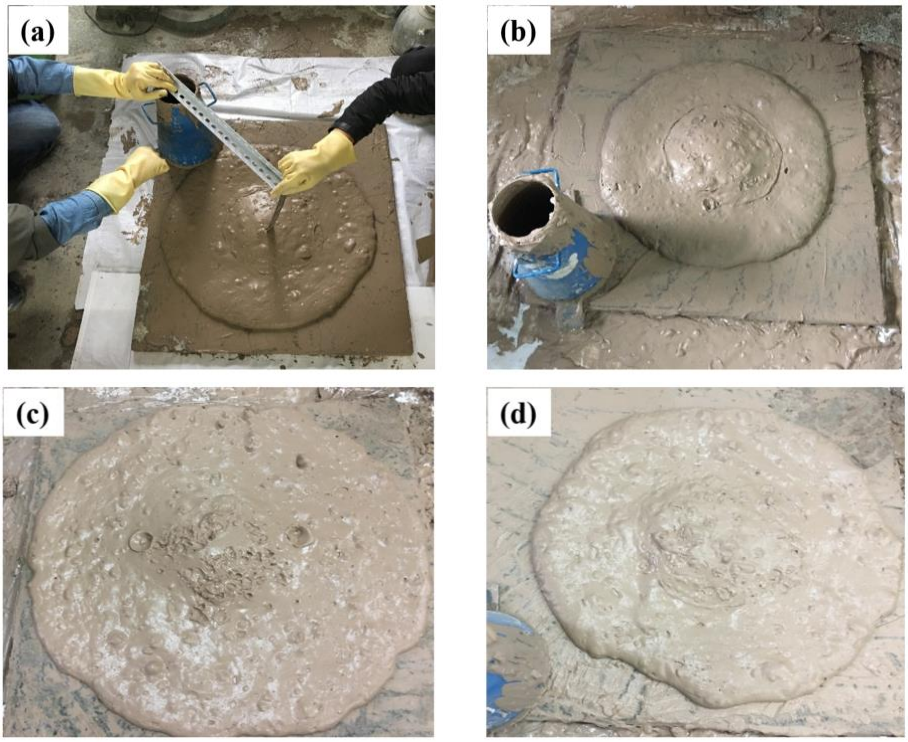

Fig. 6 The slump drop of CTB slurries: (a) c/t=1:4, SC=67wt.%; (b) c/t=1:10, SC=69wt.%; (c) c/t=1:20, SC=67wt.%; and (d) c/t=1:20, SC=69wt.%

Fig. 6 indicates the slump sharpness of CTB slurry. Slump and SC values were 27-27.6 cm and 65 wt.%, 25.7-26.6 cm and 67 wt.%, and 25-25.8 cm and 69 wt.%, for a c/t value of 1:4, 1:1 and 1:2, respectively. The intuitive expression of fluidity is the extended range of the slurry, that is, the size of the area that the slurry can cover after slump is completed. The larger the slump, the better the CTB's fluidity, but if the slump is too big, the workability is low, and segregation and bleeding are easy to occur. The results of this test show that the maximum slump value is 276 mm; the minimum slump value is 250 mm. Note that, although CPB with a high slump value is beneficial for its transportation, it also has some downside. Indeed, a high slump for a given CPB composition could lead to lower mechanical strength or higher liquefaction susceptibility of the CPB.

These results present a significant indicator when considering the flow conditions of CTB slurries at the pipeline orifices. The smaller the slump, the higher the stress application in the pipeline, which will result in fast pipe wears, blockages, and ruptures. A greater slump of the CTB slurry to be delivered into underground mined-out voids or stopes is indicative of larger mobility and will not cause any pipeline problems but will lead to longer curing times for the hardening process of the backfill mixes because of their water retentions. A clear relationship between solid content and slump consistency of backfilling should be considered when designing the pipe network properly and its travel distance to be reached in underground structures.

3.2 Backfill rheology

3.2.1 Solid content effect on the rheology of backfill

To observe the influence of c/t and SC on rheology (e.g., shear stress and viscosity) of slurries, the histograms between shear stress and solid content (SC) are obtained in Fig. 7. It is clear that, with an increase in corresponding SC values, CTB tends to indicate a greater viscosity and yield stress, but lesser flowability for a given backfill recipe. One can state that shear stress and viscosity increase with increasing SC values. Shear stress values of mortar and the SR values were basically linear when the SC was less than 69wt.%. At the time, the whole tailing slurry belongs to Bingham model, and the multiple correlation coefficients (R^2) was greater than 0.9. However, the correlation coefficient was only 0.5 when the c/t and SC values were 1:4 and 69 wt.%, indicating that it was no longer a Bingham body, and the flow ability was weak. Correspondingly, the viscosity value of the CTB slurry was between 0.2 and 0.3, and the R^2 values were larger than 0.9. However, a large fluctuation occurred when the SC and c/t values were 69 wt.% and 1:20, respectively.

As observed in underground mine operations, additional water is needed to enhance the flowability of backfill while certifying the formation of cement hydration. Indeed, water content is important because of two reasons: i) it controls the slump consistency of backfilling, and ii) it has a crucial influence on the strength gain of backfilling. The high-water content will ensure a high degree of saturation and hence lead to a better slump value. However, an increase in water can also create an undesirable impact on the strength development of filling by not getting hardened over curing time because of excessive water within the backfill. Note that a stope filled with too much water can fail by leading serious consequences such as fiscal ramifications, injuries and/or fatalities. Therefore, engineers should reach a good balance between strength and flow behavior of backfilling as a function of water.

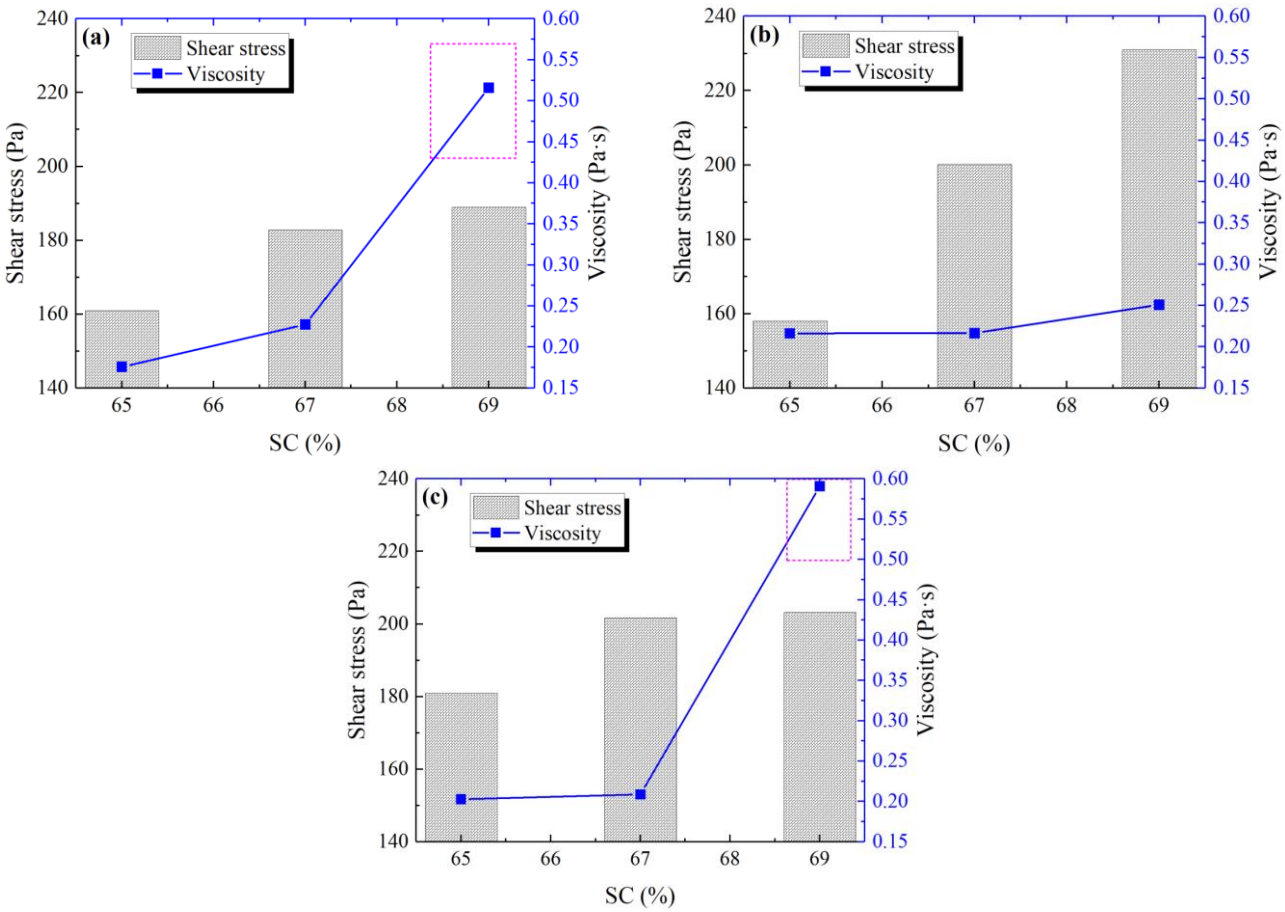

Fig. 7 Evaluation of relationships among shear stress, viscosity and solid content of backfilling: (a) c/t=1:4: (b) c/t=1:10; and (c) c/t=1:20

3.2.2 Shear rate effect on shear stress of backfill

To explore a quantitative link between shear rate and stress, the linear, exponential, logarithmic, and power function fitting methods were employed. Fig. 8 indicates the relations between the shear rate (SR) and the shear stress of backfill slurries. One can observe obviously that the shear stress increased with increasing SR. The linear fit had the highest multiple correlation coefficients (R^2). The average values of R^2 were also 0.8225, 0.9731 and 0.8837 when the c/t values were 1:4, 1:10 and 1:20, respectively. Therefore, the relationship between shear stress and stress rate for the studied filling samples can be expressed as a linear equation.

Overall, it can be stated evidently that high mixing speed can give better fluidity by affecting CTB's rheology. This is mainly because the flow behavior of such non-Newtonian and cementitious materials is believed to be triggered by the interactions of the tailings' grain size and cement hydration product. The shear action of rheological testing deteriorates the backfill structure and gives rise to the drop of the corresponding viscosity. Thus, the microstructure of the backfill slurry is too weak after enduring strong shear action induced by high mixing intensity.

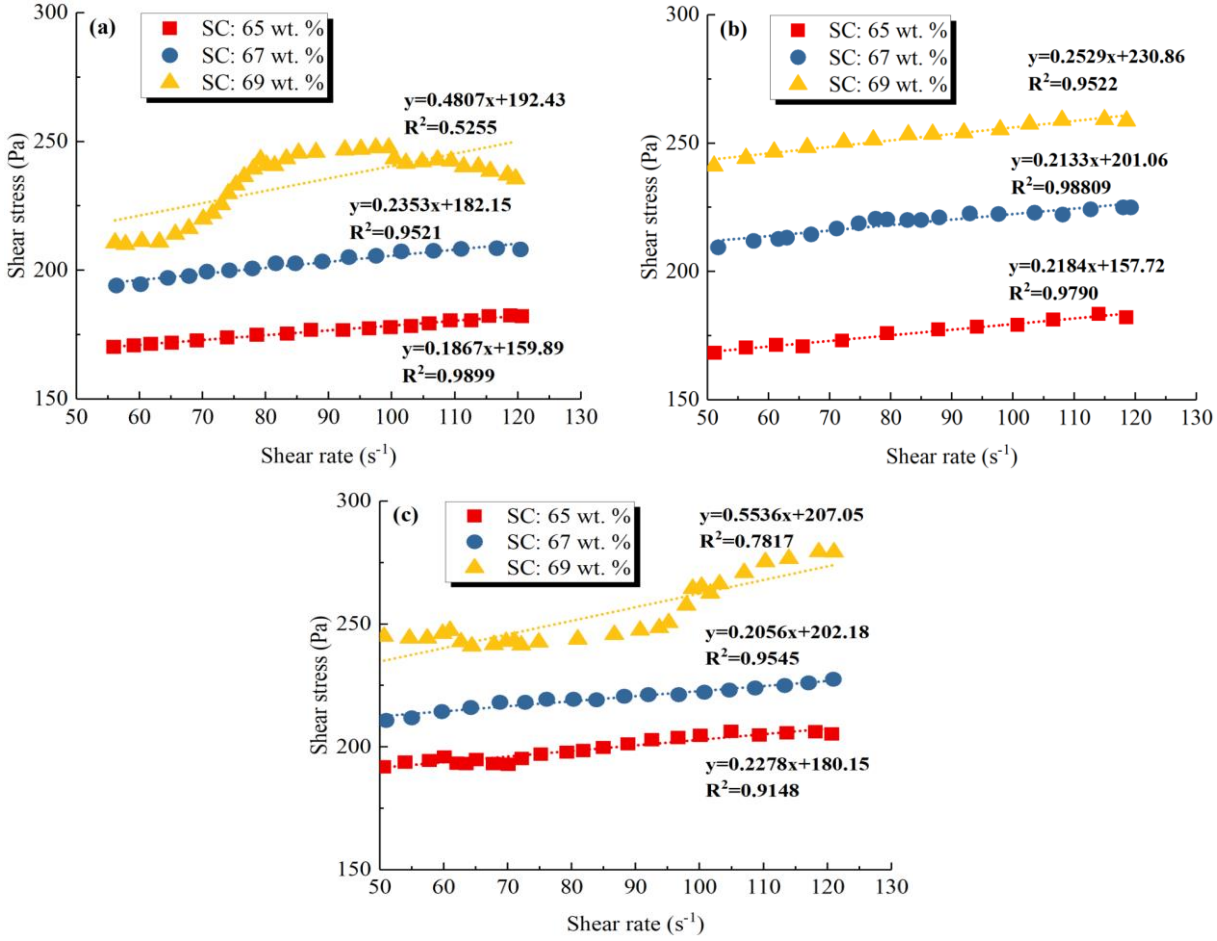

Fig. 8 Relationships between shear stress and rate of filling: (a) c/t=1:4; (b) c/t=1:10; and (c) c/t=1:20

3.3 Sedimentation behavior of CTB slurry

Overall, a steady ion layer occurs in fine grains when backfill particle size is under 15μm. As small grains are nearly the same in terms of their size, the repulsive force of a similar electric charge is higher than the attractive force. It means that grains are dispersed after a collision, and large grains are not occurred to get sedimentation quickened and remain in suspension form. This is caused by a reduction in the speed of sedimentation in the matrix. Considering a typical backfill concentration of up to 85 wt.%, grains are not settled naturally, but the interference settlement, which delays sedimentation, gives rise to a wide range of grain size. To study relationship between sedimentation rate and PAM flocculant content, the linear, exponential, logarithmic, and power function fitting methods were employed. By comparing the multiple correlation coefficients of different fitting methods, the relationship between sedimentation rate and PAM flocculant quantity is shown clearly in Fig. 9. The multiple R^2 of the linear, exponential, logarithmic, and power fitting methods are high. However, the R^2 of exponential fitting (0.9293) was the largest among others. Consequently, the relation between sedimentation rate and PAM flocculant content could be expressed as an exponential equation.

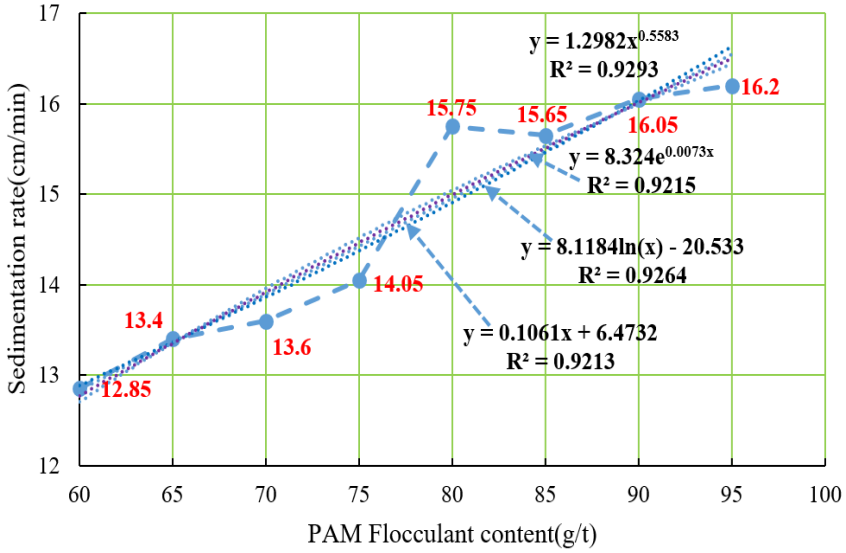

Fig. 9 Relationship between sedimentation rate and PAM flocculant content of CTB slurries

One can achieve that a key stage for the accumulation of fine grains through flocculants is the adsorption of flocculants on solid backfill surfaces. Firstly, flocculants are delivered to solid surfaces by diffusion, and, secondly, a strong connection between flocculants and solid surfaces form. For PAM flocculant, such connections are principally stemmed from bonding between H atoms and O atoms. Additionally, in the matter of cationic or anionic polymers, electrostatic attraction and salt connection may have a central role in the adsorption mechanism. Consequently, flocculants re-orientate after the adsorption process in the backfill matrix. Fundamentally, both polymer adsorption and grain flocculation happen concurrently in the CTB slurries.

Fig. 10 showed the relations between clarification layer height (CLH) and sedimentation time (ST). It was found that the sedimentation rate with a higher PAM content was substantially faster than other groups at the initial stage of CTB's sedimentation. Moreover, CLH values of 8 groups increased sharply in 1 min. However, the growth rate of CLH slowed down significantly after 1 min. The growth rates of CLH values gradually slowed down within 1 to 30 min and the growth rates became stable after 30 min. In addition, it was found from Fig. 10 (b) that when the PAM value increased from 75g/t to 80g/t, there was a very clear difference in CLH value. For example, when ST was 20 min and PAM values are 75g/t and 80g/t, the corresponding CLH values were 200 mm and 215 mm, respectively. When ST was 30 min and PAM values are also 75g/t and 80g/t, the corresponding CLH values were 203 mm and 217.5 mm, respectively. In addition, the CLH increments were 7.5% and 7.14% when the ST was 20 min and 30 min, respectively.

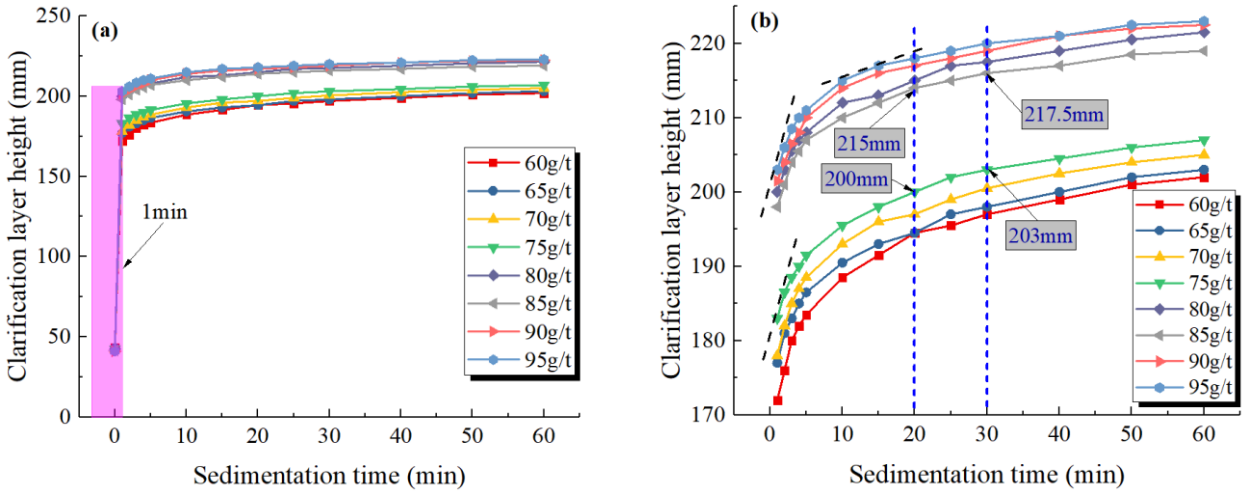

Fig. 10 Evaluation of relationships between clarification layer height and time of CTB slurries: (a) ST: 0 to 60 minutes; and (b) ST: 1 to 60 minutes

Fig. 11 showed the histogram between CLH and PAM flocculant content of CTB slurry when ST was 24 h. It was found experimentally that the CLH values were nearly the same (between 228 and 234 mm) for all samples when ST was 24 h. One can clearly observe that the sedimentation effect happens so promptly by fluctuating significantly the height of the clarification layer in a few seconds. After adding the PAM flocculant, sedimentation accelerates and needed to be drawn for 1 min.

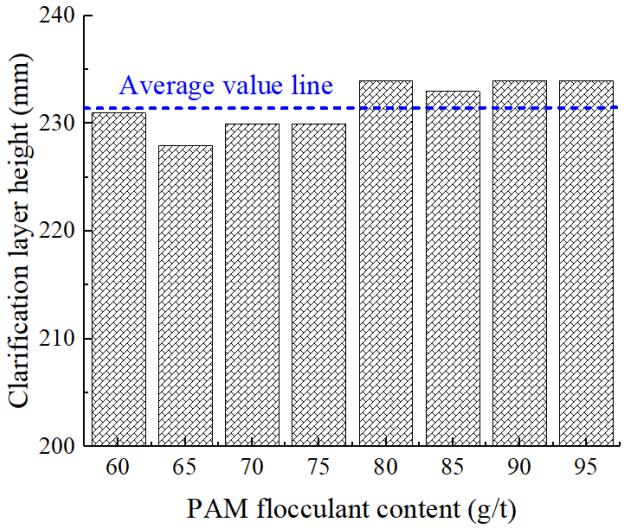

Fig. 11 Histogram between CLH and PAM flocculant content of CTB slurries at a ST of 24 hours

In addition, Figs. 12 and 13 show the process charts of flocculation sedimentation when ST was 1 minute and 24 hours, respectively. It was also found that the supernatant was still relatively turbid when the ST was 1 min, but the tailings sand floc had also enriched at the bottom of the measuring cup. But

the supernatant was very clean when the ST value was 24 h. Note that growth in the SC value of CTB slurry gives rise to a diminution of the backfill sedimentation. Frequently, the backfill sedimentation becomes slow since the supernatant liquid is turbid, and the quantity of fine grains are suspended in the supernatant and thus do not settle readily. Typically, it takes 1 min to 24 h for fine grains to fully settle down, and the supernatant is pure and uneven; CTB slurry may be re-suspended by external forces.

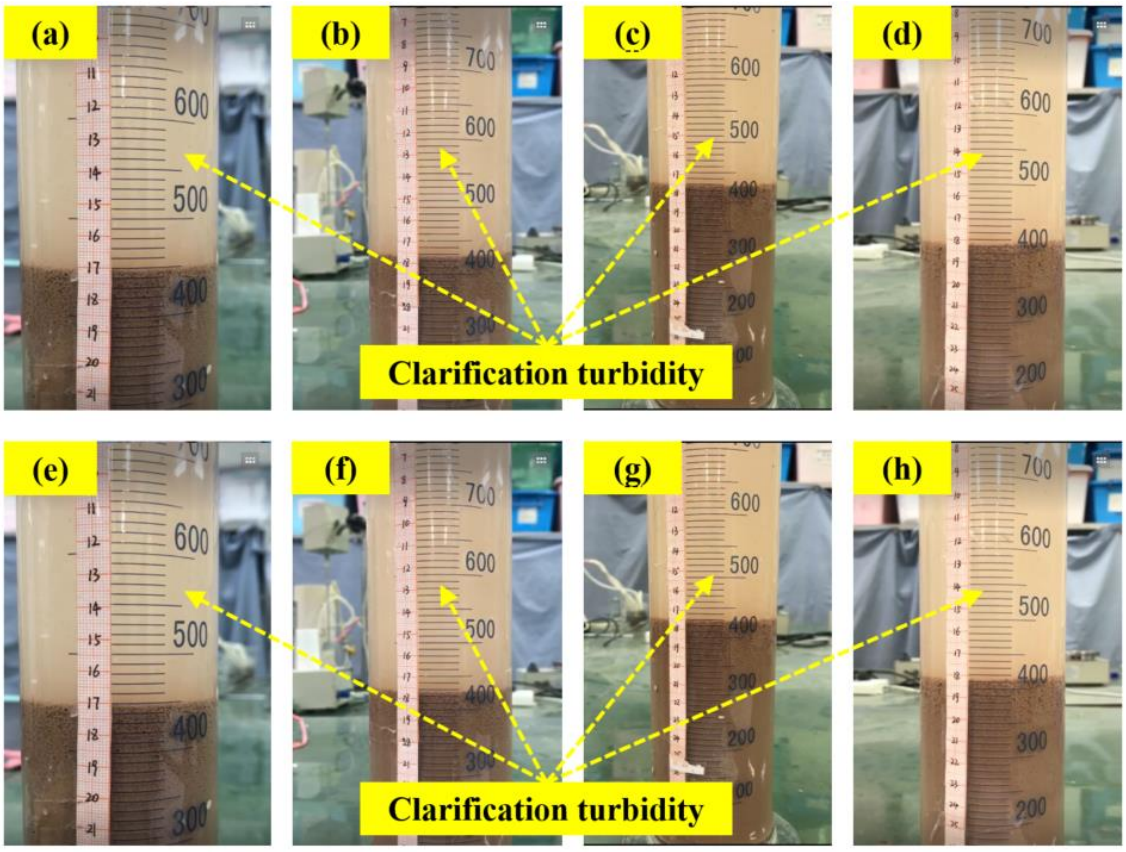

Fig. 12 Process chart of flocculation sedimentation at a ST of 1 minute:
(a) 60 g/t; (b) 65 g/t; (c) 70 g/t; (d) 75 g/t; (e) 80 g/t; (f) 85 g/t; (g) 90 g/t; and (h) 95 g/t

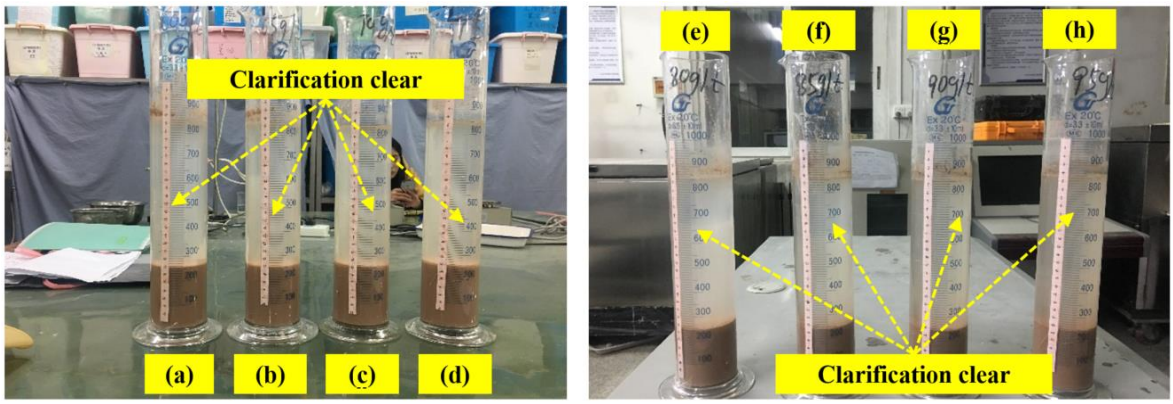

Fig. 13 Process chart of flocculation sedimentation at a ST of 24 hours:
(a) 60 g/t; (b) 65 g/t; (c) 70 g/t; (d) 75 g/t; (e) 80 g/t; (f) 85 g/t; (g) 90 g/t; and (h) 95 g/t

4 Conclusions

Various laboratory experiments on flow characteristics of the backfill slurries have been performed to explore its rheological behavior and sedimentation characteristics. The three different solid contents (e.g., 65, 67, and 69wt.%) and four different cement-to-tailings ratios (e.g., 0, 1:20, 1:10 and 1:4) were subjected to the backfill rheology. To investigate the sedimentation characteristics of CTB slurry better, polyacrylamide (PAM) was also used in the matrix as a flocculant. From the experiments performed, some interpretations are made below:

- The slump value of CTB slurry decreases as the SC values increase. Besides, the slump values decrease with rising c/t values for a given SC value.
- Shear stress and viscosity surge with increasing SC values. Relationship between shear stress and the rate is expressed as a linear equation.
- The relationship between sedimentation rate and flocculant content could be stated as an exponential equation. The sedimentation rate with a higher PAM content was significantly faster than other groups at the initial stage of the tailings sedimentation.
- When the PAM value increased from 75 to 80 g/t, there was a very clear difference in CLH. The CLH increments were also 7.5% and 7.14% when the ST was 20 min and 30 min, respectively.

In spite of these extensive laboratory results, further studies are unsurprisingly required for offering a better understanding of the field CTB slurry testing as well as the effect of temperatures on transport characteristics of the in-situ backfill slurry. A number of subjects are suggested for additional researches: (i) temperature effect on internal structure and behavior of CTB slurry, (ii) field-scale tests for better understanding the rheology of the pipeline transport considering the solid and cement contents, filling rates, admixture types and rates, and pipeline network effects, and (iii) using a fluid mechanics software to simulate the rheology, sedimentation and transport characteristics of CTB slurries.

Acknowledgements

The present research work was financially supported by the National Natural Science Foundation of China (Grant Number 51804017), the Opening Fund of State Key Laboratory of Nonlinear Mechanics (Grant Number LNM202009) and the Fundamental Research Funds for Central Universities (Grant Number FRF-TP-20-001A2). Special acknowledgements are extended to two anonymous reviewers for their constructive and helpful comments that significantly improved the quality of the manuscript.

References

[1] E.T. Asr, R. Kakaje, M. Ataei, and M.R.T. Mohammadi, *A review of studies on sustainable development in mining life cycle*, J. Clean. Prod. 229 (2019), pp. 213-231.

[2] B. Koohestani, A.K. Darban, P. Mokhtari, E. Darezereshki, E. Yilmaz, and E. Yilmaz, *Influence of hydrofluoric acid leaching and roasting on mineralogical phase transformation of pyrite in sulfidic mine tailings*, Minerals. 10 (2020), pp. 513-513.

[3] S. Cao, W.D. Song, and E. Yilmaz, *Influence of structural factors on uniaxial compressive strength of cemented tailings backfill*, Constr. Build. Mater. 174 (2018), pp. 190-201.

[4] K. Fang, and M. Fall, *Effects of curing temperature on shear behaviour of cemented paste backfill-rock interface*, Int. J. Rock Mech. Min. Sci. 112 (2018), pp. 184-192.

[5] E. Yilmaz, *Stope depth effect on field behaviour and performance of cemented paste backfills*, Int. J. Min. Reclam. Environ. 32 (2018), pp. 273-296.

[6] H.Z. Jiao, S.F. Wang, Y.X Yang, and X.M. Chen, *Water recovery improvement by shearing of gravity-thickened tailings for cemented paste backfill*, J. Clean. Prod. 245 (2020), pp. 118882-118882.

[7] E. Yilmaz, T. Belem, and M. Benzaazoua, *Study of physico-chemical and mechanical characteristics of consolidated and unconsolidated cemented paste backfills*, Miner. Resour. Manage. 29 (2013), pp. 81-100.

[8] W. Sun, H.J. Wang, and K.P. Hou, *Control of waste rock-tailings paste backfill for active mining subsidence areas*, J. Clean. Prod. 171 (2018), pp. 567-579.

[9] G.L. Xue, Yilmaz, E., W.D. Song, and S. Cao, *Fiber length effect on strength properties of polypropylene fiber reinforced cemented tailings backfill specimens with different sizes*, Constr. Build. Mater. 241 (2020), pp. 118113-118113.

[10] B. Koohestani, A.K. Darban, E. Darezereshki, P. Mokhtari, E. Yilmaz, and E., Yilmaz, *The influence of sodium and sulfate ions on total solidification and encapsulation potential of iron-rich acid mine drainage in silica gel*, J. Environ. Chem. Eng. 6 (2018), pp. 3520-3527.

[11] E. Yilmaz, A. Kesimal, and B. Ercikdi, *The factors affecting the strength and stability of paste backfill*, Yerbilimleri – Turkish Earth Sciences, 28 (2003), pp. 155-169.

[12] W. Li, and M. Fall, *Strength and self-desiccation of slag-cemented paste backfill at early ages: Link to initial sulphate concentration*, Cem. Concr. Comp. 89 (2018), pp. 160-168.

[13] S. Cao, G.L. Xue, and E. Yilmaz, *Flexural behavior of fiber reinforced cemented tailings backfill under three-point bending*, IEEE Access, 7 (2019), pp. 139317-139328.

[14] S. Cao, D. Zheng, E. Yilmaz, Z.Y. Yin, G.L. Xue, and F.D. Yang, *Strength development and microstructure characteristics of artificial concrete pillar considering fiber type and content effects*, Constr. Build. Mater. 256 (2020), pp. 119408-119408.

[15] J.P. Doherty, A. Hasan, G.H. Suazo, and A. Fourie, *Investigation of some controllable factors that impacts the stress state in cemented paste backfill*, Can. Geotech. J. 52 (2015), pp. 1901-1912.

[16] S. Cao, G.L. Xue, E. Yilmaz, Z.Y. Yin, and F.D. Yang, *Utilizing concrete pillars as an environmental mining practice in underground mines*, J. Clean. Prod. 278 (2021), pp. 123433-123433.

[17] Q. Sun, B. Li, S. Tian, C. Cai, and Y.J. Xia, *Creep properties of geopolymer cemented coal gangue-fly ash backfill under dynamic disturbance*, Constr. Build. Mater. 191 (2018), pp. 644-654.

[18] H.Q. Jiang, M. Fall, E. Yilmaz, L. Yang, and L. Ren, *Effect of mineral admixtures on flow properties of fresh cemented paste backfill: Assessment of time dependency and thixotropy*, Powder Technol. 372 (2020), pp. 258-266.

[19] D. Wu, G.H. Sun, and Y.C. Liu, *Modeling the thermo-hydro-chemical behavior of cemented coal gangue-fly ash backfill*, Constr. Build. Mater. 111 (2016), pp. 522-528.

[20] G.L. Xue, E. Yilmaz, W.D. Song, and S. Cao, *Compressive strength characteristics of cemented tailings backfill with alkali-activated slag*, Appl. Sci. 8 (2018), pp. 1537-1537.

[21] Y.P. Kou, H.Q. Jiang, L. Ren, E. Yilmaz, and YH. Li, *Rheological properties of cemented paste backfill with alkali-activated slag,* Minerals. 10 (2019), pp. 288-288.
[22] I. Alp, H. Deveci, Y.H. Sungun, A.O. Yilmaz, A. Kesimal, and E. Yilmaz, *Pozzolanic characteristics of a natural raw material for use in blended cements,* Iran. J. Sci. Tech. Trans. B: Eng. 33 (2009), pp. 291-300.
[23] L. Liu, J. Xin, C. Huan, C.C. Qi, W.W. Zhou, and K.I. Song, *Pore and strength characteristics of cemented paste backfill using sulphide tailings: Effect of sulphur content,* Constr. Build. Mater. 237 (2020), pp. 117452-117452.
[24] T. Belem, and M. Benzaazoua, *Design and application of underground mine paste backfill technology,* Geotech. Geol. Eng. 26 (2008), pp. 147-174.
[25] C.C. Qi, and A. Fourie, *Cemented paste backfill for mineral tailings management: Review and future perspectives,* Miner. Eng. 144 (2019), pp. 106025-106025.
[26] J.Y. Wu, H.W. Jing, Q. Yin, B. Meng, and G.S. Han, *Strength and ultrasonic properties of cemented waste rock backfill considering confining pressure, dosage and particle size effects,* Constr. Build. Mater. 242 (2020), pp. 118132.
[27] E. Yilmaz, T. Belem, and M. Benzaazoua, *One-dimensional consolidation parameters of cemented paste backfills,* Miner. Resour. Manage. 28 (2012), pp. 29-45.
[28] G.L. Xue, E. Yilmaz, W.D. Song, and E. Yilmaz, *Influence of fiber reinforcement on mechanical behavior and microstructural properties of cemented tailings backfill,* Constr. Build. Mater. 213 (2019), pp. 275-285.
[29] B. Yan, W. Zhu, C. Hou, E. Yilmaz, and M. Saadat, *Characterization of early age behavior of cemented paste backfill through the magnitude and frequency spectrum of ultrasonic P-wave,* Constr. Build. Mater. 249 (2020), pp. 118733-118733.
[30] S. Cao, E. Yilmaz, and W.D. Song, *Evaluation of viscosity, strength and microstructural properties of cemented tailings backfill,* Minerals, 8 (2018), pp. 352-352.
[31] C.C. Qi, Q.S. Chen, A. Fourie, J.W. Zhao, and Q.L. Zhang, *Pressure drop in pipe flow of cemented paste backfill: Experimental and modeling study,* Powder Technol. 333 (2018), pp. 9-18.
[32] G.L. Xue, E. Yilmaz, W.D. Song, and S. Cao, *Analysis of internal structure behavior of fiber reinforced cement-tailings matrix composites through X-ray computed tomography,* Comp. Part B: Eng. 175 (2020), pp. 107091-107091.
[33] X.J. Deng, B. Klein, D.J. Hallbom, and J. Zhang, *Influence of particle size on the basic and time-dependent rheological behaviors of cemented paste backfill,* J. Mater. Eng. Perform. 27 (2018), pp. 3478-3487.
[34] B. Xiao, Z.J. Wen, F. Wu, L.T. Li, Z.Q. Yang, Q. Gao, *A simple L-shape pipe flow test for practical rheological properties of backfill slurry: A case study,* Powder Technol. 356 (2019), pp. 1008-1015.
[35] S. Cao, E. Yilmaz, and W.D. Song, *Fiber type effect on strength, toughness and microstructure of early age cemented tailings backfill,* Constr. Build. Mater. 223 (2019), pp. 44-54.
[36] D. Hewitt, S. Allard, and P. Radziszewski, *Pipe lining abrasion testing for paste backfill operations,* Miner. Eng. 22 (2009), pp. 1088-1090.
[37] G.L. Xue, E. Yilmaz, W.D. Song, and S. Cao, *Mechanical, flexural and microstructural properties of cement-tailings matrix composites: Effects of fiber type and dosage,* Comp. Part B: Eng. 172 (2019), pp. 131-142.
[38] Q.L. Zhang, J.Q. Cui, J.J. Zheng, X.M. Wang, X.L. Wang, *Wear mechanism and serious wear position of casing pipe in vertical backfill drill-hole,* Transac. Nonfer. Met. Soc. China 21 (2011), pp. 2503-2507.
[39] S. Cao, E. Yilmaz, G.L. Xue, and W.D. Song, *Assessment of acoustic emission and triaxial mechanical properties of rock-cemented tailings matrix composites,* Adv. Mater. Sci. Eng. 2019, pp. 6742392-6742392.
[40] Y.Y. Tan, X. Yu, D. Elmo, L.H. Xu, and W.D. Song, *Experimental study on dynamic mechanical property of cemented tailings backfill under SHPB impact loading,* Int. J. Miner. Metal. Mater. 4 (2019), pp. 404-416.
[41] S. Cao, E. Yilmaz, G.L. Xue, E. Yilmaz, and W.D. Song, *Loading rate effect on uniaxial compressive*

480 *strength behavior and acoustic emission properties of cemented tailings backfill,* Constr. Build. Mater. 213
481 (2019), pp. 313-324.
482 [42] K. Zhao, X. Yu, S.T. Zhu, Y. Zhou, Q. Wang, and J.Q. Wang, *Acoustic emission investigation of cemented*
483 *paste backfill prepared with tantalum-niobium tailings,* Constr. Build. Mater. 237 (2020), pp.
484 117523-117523.
485 [43] M. Benzaazoua, T. Belem, and E. Yilmaz, *Novel lab tool for paste backfill,* Can. Min. J. 127 (2006), pp.
486 31-31.
487 [44] H.Q. Jiang, J. Han, Y. Li, E. Yilmaz, Q. Sun, and J. Liu, *Relationship between ultrasonic pulse velocity and*
488 *uniaxial compressive strength for cemented paste backfill with alkali-activated slag,* Nondestruct. Test. Eva.,
489 (2019), DOI: 10.1080/10589759.2019.1679140.
490 [45] D. Wu, Y.L. Zhang, and Y.C. Liu, *Mechanical performance and ultrasonic properties of cemented gangue*
491 *backfill with admixture of fly ash,* Ultrasonics, 64 (2016), pp. 89-96.
492 [46] W.B. Xu, Q.L. Li, and B. Liu, *Coupled effect of curing temperature and age on compressive behavior,*
493 *microstructure and ultrasonic properties of cemented tailings backfill,* Constr. Build. Mater. 237 (2020), pp.
494 117738-117738.
495 [47] W. Sun, K.P. Hou, Z.Q. Yang, and Y.M. Wen, *X-ray CT three-dimensional reconstruction and discrete*
496 *element analysis of the cement paste backfill pore structure under uniaxial compression,* Constr. Build.
497 Mater. 138 (2017), pp. 69-78.
498 [48] H.Q. Jiang, H.S. Yi, E. Yilmaz, S.W. Liu, and L.P. Qiu, *Ultrasonic evaluation of strength properties of*
499 *cemented paste backfill: Effect of mineral admixture and curing temperature,* Ultrasonics, 100 (2020), pp.
500 105983-105983.
501 [49] P. Wang, N. Gao, K. Ji, L. Stewart, and C. Arson, *DEM analysis on the role of aggregates on concrete*
502 *strength,* Comp. Geotech. (2019), pp. 103290-103290.
503 [50] S. Panchal, D. Deb, and T. Sreenivas, *Variability in rheology of cemented paste backfill with hydration age,*
504 *binder and superplasticizer dosages,* Adv. Powder Technol. 29 (2018), pp. 2211-2220.
505 [51] X.J. Deng, J.X. Zhang, B. Klein, N. Zhou, and B. de Wit, *Experimental characterization of the influence of*
506 *solid components on the rheological and mechanical properties of cemented paste backfill,* Int. J. Miner.
507 Process. 168 (2017), pp. 116-125.
508 [52] H.Q. Jiang, M. Fall, and L. Cui, *Yield stress of cemented paste backfill in sub-zero environments:*
509 *Experimental results,* Miner. Eng. 92 (2016), pp. 141-150.
510 [53] J. Bian, M. Fall, and S. Haruna, *Sulfate-induced changes in rheological properties of fibre-reinforced*
511 *cemented paste backfill,* Mag. Concr. Res. (2019), https://doi.org/10.1680/jmacr.19.00311.
512 [54] H.Q. Jiang, and M. Fall, *Yield stress and strength of cemented tailings backfill in sub-zero environments:*
513 *slag-paste backfill,* J. Sustain. Cement Mater. 6 (2017a), pp. 314-331.
514 [55] H.Q. Jiang, and M. Fall, *Yield stress and strength of cemented tailings backfill in sub-zero environments:*
515 *Portland cement paste backfill,* Int. J. Miner. Process. 160 (2017b), pp. 68-75.
516 [56] D. Wu, M. Fall, and S.J. Cai, *Coupling temperature, cement hydration and rheological behaviour of*
517 *cemented paste backfill structures,* Miner. Eng. 42 (2013), pp. 76-87.
518 [57] D.L. Li, D.M. Wang, C.F. Ren, and Y.F. Rui, *Investigation of rheological properties of fresh cement paste*
519 *containing ultrafine circulating fluidized bed fly ash,* Constr. Build. Mater. 188 (2018), pp. 1007-1013.
520 [58] W.N. Meng, A. Kumar, and K.H. Khayat, *Effect of silica fume and slump-retaining polycarboxylate-based*
521 *dispersant on the development of properties of Portland cement paste,* Cem. Concr. Comp. 99 (2019), pp.
522 181-190.
523 [59] Y. Peng, and S. Jacobsen, *Influence of water/cement ratio, admixtures and filler on sedimentation and*
524 *bleeding of cement paste,* Cem. Concr. Res. 54 (2013), pp. 133-142.
525 [60] B. Feneuil, N. Roussel, and O. Pitois, *Yield stress of aerated cement paste,* Cem. Concr. Res. 127 (2020), pp.

105922-105922.
[61] Y.Q. Guo, T.S. Zhang, J.X. Wei, Q.J. Yu, and S.X. Ouyang, *Evaluating the distance between particles in fresh cement paste based on the yield stress and particle,* Constr. Build. Mater. 142 (2017), pp. 109-116.
[62] L. Yang, W. Xu, E. Yilmaz, Q. Wang, and J. Qiu, *A combined experimental and numerical study on the triaxial and dynamic compression behavior of cemented tailings backfill,* Eng. Struct. 219 (2020), pp. 110957-110957.
[63] C.R. Wu, and S.C. Kou, *Effects of high calcium sepiolite on the rheological behaviour and mechanical strength of cement pastes and mortars,* Constr. Build. Mater. 196 (2019), pp. 105-114.
[64] P. Xiaopeng, M. Fall, and S. Haruna, *Sulphate induced changes of rheological properties of cemented paste backfill,* Miner. Eng. 141 (2019), pp. 105849-105849.
[65] S. Haruna, and M. Fall, *Time and temperature-dependent rheological properties of cemented paste backfill that contains superplasticizer,* Powder Technol. 360 (2020), pp. 731-740.
[66] Y.R. Zhang, X. Luo, X.M. Kong, F.Z. Wang, and L. Gao, *Rheological properties and microstructure of fresh cement paste with varied dispersion media and superplasticizers,* Powder Technol. 330 (2018), pp. 219-227.
[67] D. Ouattaraa, A. Yahia, M. Mbonimpa, and T. Belem, *Effects of superplasticizer on rheological properties of cemented paste backfills,* Int. J. Miner. Process. 161 (2017), pp. 28-40.
[68] K.K. Sun, S.P. Wang, L. Zeng, and X.Q. Peng, *Effect of styrene-butadiene rubber latex on the rheological behavior and pore structure of cement paste,* Comp. Part B: Eng. 163 (2019), pp. 282-289.
[69] E.G. Aldama, M. Mayorga, J.C.A. Arcos, and L.R. Salazar, *Rheological behavior of cement paste added with natural fibres,* Constr. Build. Mater. 198 (2019), pp. 148-157.
[70] M. Azima, and Z.B. Bundur, *Influence of sporasarcina pasteurii cells on rheological properties of cement paste,* Constr. Build. Mater. 225 (2019), pp. 1086-1097.
[71] D. Feys, and A. Asghari, *Influence of maximum applied shear rate on the measured rheological properties of flowable cement pastes,* Cem. Concr. Res. 117 (2019), pp. 69-81.
[72] D.W. Jiao, C.J. Shi, and Q. Yuan, *Influences of shear-mixing rate and fly ash on rheological behavior of cement pastes under continuous mixing,* Constr. Build. Mater. 188 (2018), pp. 170-177.
[73] D. Zheng, W.-D. Song, Y.-Y. Tan, S. Cao, Z.-L. Yang, and L.-J. Sun, *Research on fractal and microscopic quantitative characterization of unclassified tailings flocs,* Int. J. Miner. Metall. Mater. (2020), https://doi.org/10.1007/s12613-020-2181-2.
[74] Y.X. Ke, X.M. Wang, and Q.L. Zhang, *Flocculating sedimentation characteristic of pre-magnetized crude tailings slurry,* Chin J. Nonferr. Met. 27 (2017), pp. 392-398.
[75] L. Wang, J.C. Li, and J.F. Zhou, *Numerical study of flocculation settling of cohesive sediment,* Acta. Phys. Sin. 59 (2010), pp. 3315-3323.
[76] Z. Yang, Q. Gao, D. Chen, and S. Wu, *Backfilled starting modes and pipeline resistance of mixed slurry prepared with waste rocks and tailings,* J. Wuhan Inst. Tech. 38 (2016), pp. 369-375.
[77] S. Yin, A. Wu, K. Hu, Y. Wang, and Y. Zhang, *The effect of solid components on the rheological and mechanical properties of cemented paste backfill,* Miner. Eng. 35 (2012), pp. 61-66.
[78] C. Dai, A. Wu, Y. Qi, Z. Chen, and B. Li, *Mechanical properties of paste slurry under constant shear rate in initial structure failure process,* Adv. Mater. Sci. Eng. (2019), pp. 2971563-2971563.
[79] W. Xu, M.M. Tian, Q.L. Li, *Time-dependent rheological properties and mechanical performance of fresh cemented tailings backfill containing flocculants,* Miner. Eng. 145 (2020), pp. 106064-106064.
[80] D.Q. Deng, L. Liu, Z.L. Yao, K.I.-I.L. Song, and D.Z. Lao, *A practice of ultra-fine tailings disposal as filling material in a gold mine,* J. Environ. Manage. 196 (2017), pp. 100-109.
[81] V.L. Petra, and V.B. David, *Yield stress measurements with the vane,* J. Non-Newton. Fluid Mech. 63 (1996), pp. 235-261, 1996.